



The influence of Geocell Geometry on Reinforced Soil Bearing Capacity

N. Valinezhad¹, M. Ghazavi²

1- PhD candidate, K. N. Toosi University of Technology

2- Professor, K. N. Toosi University of Technology, Department of Civil Engineering

nsvalinezhad@gmail.com

Abstract

Geocell reinforced soil is a cellular mattress with an almost honeycombed configuration. The Geocell reinforcement not only increase the soil bearing capacity but also reduce its settlement. There is little information on interaction effects of its geometry parameters. This paper discusses the trends of footing behavior in terms of Bearing Capacity Ratio (BCR). Several different configurations of geocell were examined. The obtained results show a slight interaction between the length of the Geocell layer and the required cover layer thickness. The most significant parameter is find to be the Geocell height. Although the optimum dimension for the height, length and aperture size of the cells is obtained.

Keywords: Geocell, Reinforcement, Bearing Capacity, Sand.

1. INTRODUCTION

One of the most effective approaches to reduce footing load effects transmitted to the soft underlying soils is to improve its stiffness. Among various available methods, the latest invention to enhance the stiffness is to maintain the confinement of the overlying layers using Geocell [J. S. Vinod et al., 2011]. Geocells originally were developed by the U.S. Army COE to improve vehicular mobility over loose sandy subgrade (Webster and Alford 1978). Geocell is a term used for cells with honeycomb configuration in which the soil would be encapsulated. The three dimensional structure of the pockets cause interconnection effects which produce a wide cushion and also prevents lateral spreading of the infill soil by additional confinement. So, by using the Geocells, the confined soil can carry the footing loads thorough the tension strength of Geocell polymeric cell walls and the resulted mattress spread the loads over a wider flat. This phenomena leads to an improvement in the foundation overall efficiency. There are several investigations in which the Geocell reinforcement beneficence is reported [Krishnaswamy et al., 2000; Dash et al., 2003, 2004; Latha et al., 2006; Sireesh et al., 2009; MoghaddasTafreshi and Dawson, 2010, 2012; Yang et al., 2012; Leshnisky and Ling, 2013]. A conventional triaxial apparatus has been used widely to investigate the shear strength of sand reinforced by single and multiple geocell arrangements (Rajagopal et al. 1999; Mengelt et al. 2006; Tafreshi and Dawson 2010; Biswas et al. 2013). The improved performance of sand reinforced by geocells was attributed to the apparent cohesion between the granular material and the geocell strips (Bathurst and Karpurapu 1993). The role of cyclic loads under triaxial conditions has been investigated to examine how reinforced granular media behave under various geotechnical and pavement applications (Tseng and Lytton 1989; Cowland and Wong 1993; Sekine et al. 1994; Haque et al. 2004; Kwon and Tutumluer 2009; Palmeira and Antunes 2010; Al-Qadi et al. 2012; Yang et al. 2012; Leshchinsky and Ling 2013; Indraratna and Nimbalkar 2013; Santos et al. 2013). However, only limited studies have investigated the behavior of granular material under a plane-strain environment that is applicable for rail tracks (Peters et al. 1988; Radampola 2006; Radampola et al. 2008; Wanatowski et al. 2008; Choudhury 2009). The purpose of the present study is to analyze, by the aid of Design Of Experiment, the influencing parameters of geocell reinforced sand under strip footing and in turn of interaction effects between geometry parameters. A series of model tests on strip footing supported on geocell reinforced sand bed are carried out. The four influencing parameters varied for the statistical analysis are cover layer thickness, u , Geocell height, h , cell aperture size, d , and length, b , of geocell layer. The parameters are defined in a dimensionless form by dividing to footing width, B .



2. PROBLEM DEFINITION

The strip footing with the width of B is placed on the horizontal surface of geocell reinforced dry sand. The magnitude of the ultimate bearing pressure of the footing in different settlement ratios is to be determined. The geometry of the problem is illustrated in fig.1. in which the geocell height, cell aperture size, soil cover thickness (soil between the footing and geocell layer) and the length of the layer, are denoted by h , d , u and b alternatively.

The footing with the width of B is placed on the horizontal surface of geocell reinforced dry sand. The magnitude of the ultimate bearing pressure of the footing in different settlement ratios is to be determined. The geometry of the problem is illustrated in fig.1. in which the geocell height, cell aperture size, soil cover thickness (soil between the footing and geocell layer) and the length of the layer, are denoted by h , d , u and b alternatively.

The quantification of the tests is done using non-dimensional factor i.e., Bearing Capacity Ratio (BCR).

$$BCR = \frac{q_{rnf}}{q_{urnf}} \quad (1)$$

In which q_{rnf} and q_{urnf} are the bearing pressure of reinforced and unreinforced sand respectively.

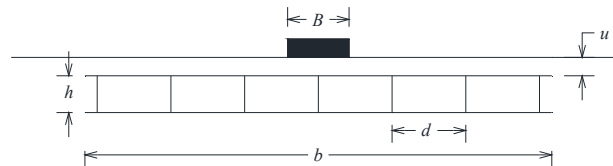


Figure 1. Schematic geometry of the problem

3. EXPERIMENTAL MODEL

A rectangular tank of size 100 cm (length) \times 55.5 cm (width) \times 70 cm (depth) was chosen. A steel footing of size 10 cm (width) \times 55 cm (length) \times 3.0 cm (thickness) is selected. The base of the footing was made sufficiently rough by cementing a thin layer of sandpaper to it using epoxy resin. The size of the footing is scaled down by 10 times the length of the tank to minimize the boundary effect. Plane strain conditions considered in the test setup by placing the length of the footing parallel to the width of the tank. The load is applied by a displacement controlled pneumatic jack via a vertical shaft in between a groove placed on top of the footing. A 10 cm LVDT is placed on the upper surface of the footing in order to monitor the vertical displacement. The load-deformation of the footing is recorded by an acquisition system including a data logger and a computer. The sand is poured into the box using a pouring system which is calibrated to obtain a desired relative density. The sidewall friction effects is minimized by coating the walls with lubricant oil. Each test preparation and conduction takes about 8 hours to done.

3. MATERIAL PROPERTIES AND SAMPLE PREPARATION

The Firouzkouh sand, type 161 is selected for test bed. The sand is classified as poorly graded sand (SP) as per the Unified Classification System. The Geocell is fabricated from high-density polyethylene geomembrane sheet of 1.5 mm wall thickness. The properties of the sand and Geocell material are mentioned in table 1. The sand is poured inside the tank evenly at 10 cm intervals. Some calibration efforts is done to achieve a relative density of 65% for the sand bed.

Table 1- The properties of the test material

Firouzkouh No. 161 Sand				Geocell			
parameter	notation	unit	value	parameter	notation	unit	value
Minimum prosity	e_{min}	-	0.53	Tear resistance	T_r	N	160
Maximum prosity	e_{max}	-	0.908	Thickness	t	mm	1.5
Specific gravity	G_s	-	2.63	Mass per unit area	μ_A	g/cm^3	0.939



Effective grain size	D ₁₀	mm	0.16	Tensile at 9% strain	T	kN/m	22
Median grain size	D ₅₀	mm	0.25				
Uniformity Coef.	C _u	-	2.5				
Curvature Coef.	C _c	-	1.6				

4. TESTS PROCEDURE

The Design Of Experiments (DOE) method not only has the advantage of structuring the experimental steps in view of minimizing the number of tests to be performed, but also considers the interaction between variables. The Response Surface Methodology, RSM, is one of DOE methods. It is a set of mathematical and statistical techniques for empirical model building [Box and Draper, 1987]. In the present study, the experiments were designed based on a Central Composite Design (CCD) five-level RSM design [5]. The commercial software, Minitab was applied. The cell height, soil cover, Geocell layer length and cell aperture size were selected as the four process-independent input variables. Table 2 shows the process input variables and the five experimental design levels (from -2 to +2) illustrated with coded and actual values, while Table 3 shows the designed test series with the measured values of the BCRs in different settlement ratios.

Table 2. Four independent parameters

Factor	Parameters	Coded values				
		-2	-1	0	1	2
A	h/B	0.2	0.6	1	1.4	1.8
B	u/B	0.1	0.2	0.3	0.4	0.5
C	b/B	2	4	6	8	10
D	d/B	0.4	0.7	1	1.3	1.6

Table 3: Test series and output results

N. tests	A	B	C	D	BCR at settlement ratio of				
					5%	10%	15%	20%	25%
1	0	-2	0	0	1.33	1.45	1.85	2.14	2.35
2	1	1	-1	1	1.61	1.64	1.97	2.28	2.46
3	0	0	2	0	1.44	1.54	2.00	2.51	2.91
4	0	0	0	-2	1.59	1.72	2.23	2.79	3.19
5	1	-1	1	-1	1.87	2.03	2.65	3.32	3.93
6	1	-1	1	1	1.64	1.79	2.30	2.85	3.33
7	-1	1	1	-1	1.27	1.39	1.71	1.90	1.98
8	1	1	1	-1	1.83	1.97	2.63	3.30	3.82
9	-1	-1	-1	-1	1.40	1.54	1.81	1.98	2.04
10	1	1	1	1	1.57	1.73	2.24	2.76	3.13
11	1	1	-1	-1	1.85	2.06	2.70	3.35	3.88
12	0	0	0	0	1.38	1.42	1.82	2.24	2.56
13	-1	-1	-1	1	1.21	1.34	1.62	1.71	1.81
14	1	-1	-1	-1	1.85	2.03	2.51	3.05	3.52
15	2	0	0	0	1.77	1.96	2.60	3.37	4.03
16	-1	-1	1	-1	1.33	1.44	1.85	2.27	2.51
17	0	0	-2	0	1.35	1.50	1.78	1.93	1.98
18	0	0	0	0	1.53	1.55	1.93	2.31	2.60
18-2	0	0	0	0	1.48	1.54	1.89	2.28	2.59
19	0	2	0	0	1.26	1.35	1.72	1.98	2.06
20	-1	-1	1	1	1.32	1.40	1.60	1.64	1.71
21	0	0	0	0	1.21	1.41	1.83	2.26	2.55
22	1	-1	-1	1	1.49	1.71	2.11	2.46	2.69
23	-1	1	1	1	1.22	1.35	1.61	1.70	1.75
24	0	0	0	2	1.45	1.56	1.77	1.95	2.05
25	-1	1	-1	1	1.27	1.37	1.63	1.74	1.80
26	-1	1	-1	-1	1.37	1.49	1.79	1.95	2.06
27	-2	0	0	0	1.05	1.13	1.22	1.25	1.31



5. RESULTS AND DISCUSSION

In order to evaluate the importance of one or more factors by comparing the response variable mean values at different factor levels one performs analysis of variance (ANOVA). The interaction of the variables and the main influencing factors is distinguished from ANOVA. In figure 2, the interaction between parameters in “BCR in s/B 25%” response is shown. In each graph, the mean value of BCR 25% response is plotted against coded value of desired input parameter. In an interaction plot the greater the departure of the lines from the parallel state means the higher the degree of interaction. The plots 2.c, 2.e. and 2.f. illustrate that larger the aperture size of the geocell pockets, lower bearing capacity.

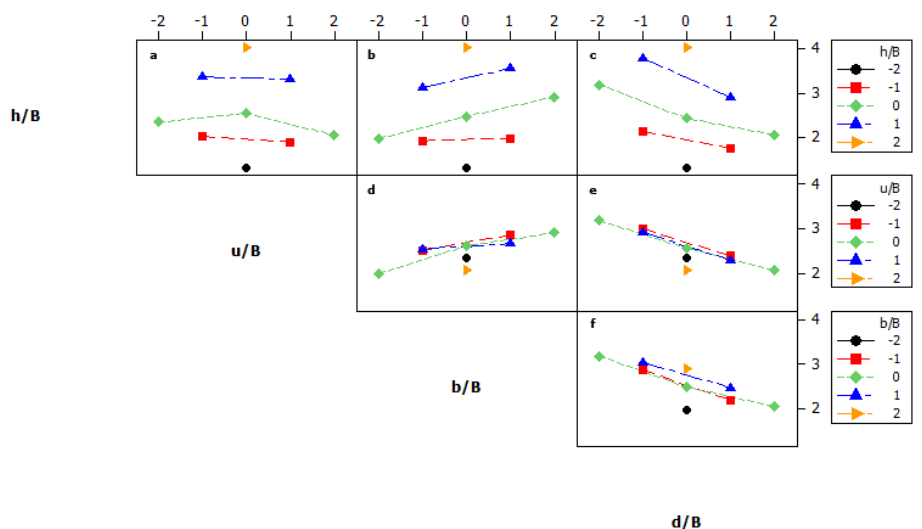


Figure 2. Interaction graphs of input parameters for “BCR in s/B=25%”

In Figure 3, the response mean values at each level of a factor are connected to one another with a line (Main effects plot). The steeper the slope of the plot line, the greater the magnitude of the desired main effect. According to plot 3.a. the BCR response increases about 4 times when you move from the low level to the high level of reinforced layer height. Therefore let’s say the height of the geocell layer has a significant influence on the BCR.

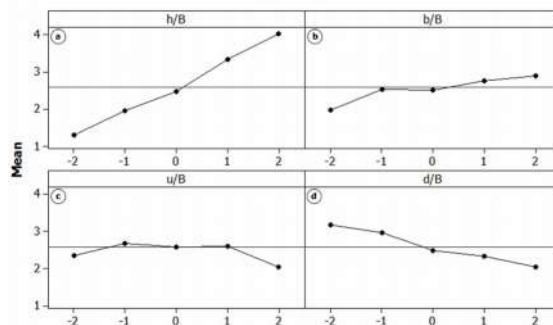


Figure 3. Main effects plot for settlement ratios (s/B) of 25%

6. REGRESSION MODEL



A polynomial approximation of the response is generally defined to express the response function on the basis of obtained data. Assume that the true response, Y , of a system depends on two coded controllable input variables, x_1 and x_2 . In case of quadratic response function with two variables, the polynomial reads as (Myers and Montgomery, 1995):

$$Y = \beta_0 + \beta_1 x_1 + \beta_2 x_2 + \beta_{12} x_1 x_2 + \beta_{11} x_1^2 + \beta_{22} x_2^2 \quad (2)$$

where x_i are dimensionless parameters and β_{ij} are regression coefficients. Using Minitab software, the values of the results of test series is inserted as input data. After DOE-RSM analysis, the relation for BCR corresponding to $s/B = 25\%$ is obtained as:

$$BCR = 2.59 + 0.69 \frac{h}{B} + 0.15 \frac{b}{B} - 0.306 \frac{d}{B} - 0.125 \frac{h}{B} \times \frac{d}{B} \quad (3)$$

Eq. (3) states that the effect of geocell layer height is the most and negative influence of the aperture size is more than the interaction term of $h/B \times d/B$.

7. DESIGN GRAPHS

Using RSM methodology, the fitted model can be represented with a surface in which two factors alter while the others remain fixed at a desired value. The response is generated in 3rd axis according to corresponding altering factors. Figure 4 illustrates the surface response of BCR ($s/B=25\%$) vs. the effective parameters. According to fig. 4a. the response takes a steep trend by increasing the h/B factor after uncoded value of 0 and decreasing the d/B beyond the uncoded value of 0. This trend is the same in fig. 4b. for h/B factor and increasing value of b/B from 0 to 2 uncoded value.

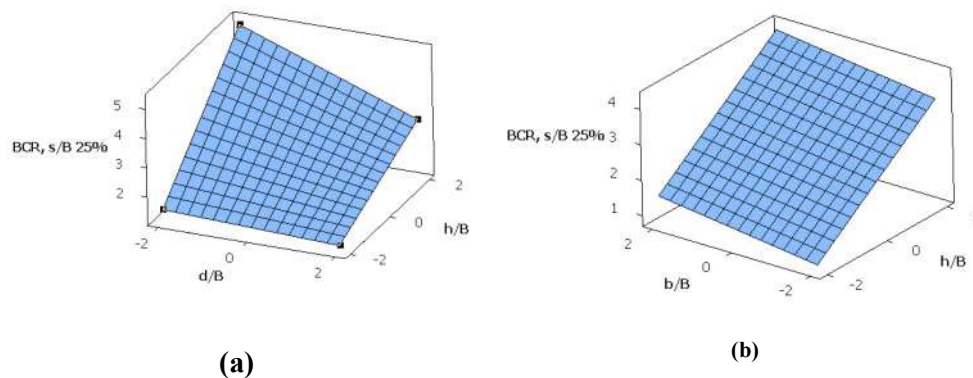
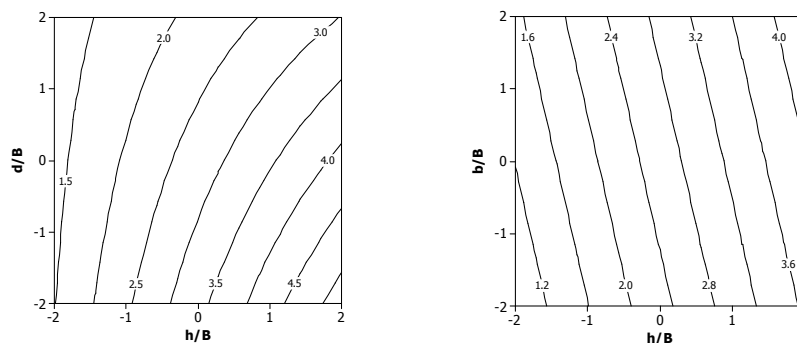


Figure 4. Variation Plot of BCR in Surface shape: BCR of $s/B = 25\%$ vs (a) d/B , h/B and (b) b/B , h/B

In Figure 5, contour plots display the three-dimensional relationship of response surface in two dimensions. Graph 5.a. shows the contour with h/B and d/B factors (predictors) plotted on the x- and y-scales and response values represented by contours. In this figure the b/B factor, holds on its optimum value which is the coded value of 1, i.e. $b/B = 8$ (table2). The pattern of the lines reveals the interaction term in the fitted model.





(a)

(b)

Figure 5. Contour of BCR of $s/B=25\%$ vs. (a) h/B , d/B (assumed $b/B = 1$), (b) h/B , b/B (assumed $d/B = 0$)

8. CONCLUSIONS

From DOE of Geocell reinforced sand the following conclusions can be drawn:

- DOE turns out to be useful to visualize and generalize parameter trends, even for such a complex behavior of altering four parameters at the same time.
- Increasing the geocell height has the most effect on overall behavior in comparison with its length and aperture size. The optimum value of height is about 1 – 1.4 times the footing width.
- A cover thickness of about 0.3 times of footing width is sufficient to just play a protector role for not rupturing the geocell walls and it doesn't improve the foundation bearing capacity.
- The length of the Geocell layer of about 8 times the footing width is sufficient and beyond this value there isn't a significant improvement.
- The aperture size of the cell pockets of about 0.7 times the footing width is appropriate to not decreasing the improvement effect.

The RSM is a local analysis and beyond the ranges of the factors, the results are invalid.

9. REFERENCES

1. L. M. Lye, DESIGN OF EXPERIMENTS IN CIVIL ENGINEERING, Annual Conference of the Canadian Society for Civil Engineering, Montréal, Québec, Canada, June 5-8, 2002.
2. G. L. SivakumarBabu and Amit Srivastava, Response Surface Methodology (RSM) in the Reliability Analysis of Geotechnical Systems, The 12th International Conference of International Association for Computer Methods and Advances in Geomechanics (IACMAG) 1-6 October, 2008, Goa, India.
3. Wojciech Pua and Jerzy Bauer, Application of the response surface method, Probabilistic Methods in Geotechnical Engineering CISM Courses and Lectures Volume 491, 2007, pp 147-168.
4. Jiju Antony, Design of Experiments for Engineers and Scientists, Butterworth and Heinemann; 2003
5. Montgomery DC. Design and analysis of experiments. New York: John Wiley; 2009.
6. Myers RH, Montgomery DC. Response surface methodology: process and product optimization using designed experiments. New York: Wiley; 1995.
7. David W. Coit, Practical Guide to Experimental Design, IIE Transactions, 1997, Volume 29, Issue 12, pp 1083-1084.
8. L. M. Lye, Design of experiments in civil engineering: Are we still in the 1920's?, Annual conf. of the Canadian Society for Civil Engineering CSCE, Montreal, Quebec, 2002.
9. Latha GM, Rajagopal K, Krishnaswamy NR. (2006), "Experimental and theoretical investigations on geocell-supported embankments". Int J Geomech; 6(1):30-5.
10. Krishnaswamy NR, Rajagopal K, Latha GM. (2000), "Model studies on geocell supported embankments constructed over a soft clay foundation". Geotech Test J; 23(1):45-54.
11. Khuri AI, Cornell JA. Response surfaces design and analysis. New York: Marcel Dekker; 1996.
12. Moghaddas Tafreshi S.N. and A.R. Dawson, Behaviour of footings on reinforced sand subjected to repeated loading – Comparing use of 3D and planar geotextile, Geotextiles and Geomembranes 28 (2010) 434-447
13. Madhavi Latha G, Dash S K, Rajagopal K., (2009) Numerical simulation of the behavior of geocell reinforced sand in foundations. International Journal of Geomechanics, ASCE, 9(4): 143-152.
14. Cherubini, C. (2000). "Reliability evaluation of shallow foundation bearing capacity on C' , ϕ' soils." Can. Geotech. J., 37, 264-269.



15. Baecher G. B., Christian J. T. 2003. Reliability and statistics in geotechnical engineering. Chichester, John Wiley publications, New York.
16. SivakumarBabu G. L., Amit Srivastava 2007. Reliability analysis of allowable pressure on shallow foundation using response surface method, Computers and Geotechnics, Elsevier Ltd., 34, 187-194.
17. R. Bahloul, A. Mkaddem, Ph. Dal Santo, A. Potiron, Sheet metal bending optimisation using response surface methodnumerical simulation and design of experiments, International Journal of Mechanical Sciences 48 (2006) 991–1003
18. Moradi M, Ghoreishi M, Torkamany MJ. Modeling and optimization ofNd:YAG laser–TIG hybrid welding of stainless steel. Lasers Eng (Submittedfor publication).
19. Minitab software, Minitab® 16.2.0, user’s guide, technical manual, 2012.